



# FEA Analysis of S-PMSG for Aircraft Application

Bharathi Thangaraj<sup>1</sup>, Deepak Arumugam<sup>2</sup>, Gomathi Somasundaram<sup>3</sup>

<sup>1</sup> Assistant Professor, Vel Tech Dr.RR & Dr.SR University, Chennai, India.

<sup>2</sup> Associate Professor, <sup>3</sup> Assistant Professor, <sup>2,3</sup> St Joseph's Institute of Technology, Chennai, India.

\*Corresponding Author Email: <sup>2</sup>adeepakceg@gmail.com

## Abstract

In this work the performance analysis of Spoke type Permanent Magnet Synchronous Generator (S-PMSG) also called buried type PMSG is presented for aircraft application. The analytical design of the generator is carried out using design equations and it is verified by RMxprt software. The simulation analysis of the generator is performed by finite element analysis software. The coupled transient electromagnetic field and thermal analysis of the generator is carried out to find the load voltage, load current, cogging torque, heat generation and thermal heat flow. Finally, the overall performance of the analytically designed generator is compared with the simulation results.

**Keywords:** Aircraft, Permanent Magnet Synchronous Generator (PMSG), Spoke Type PMSG, Finite element analysis, electromagnetic field and thermal analysis.

## 1. Introduction

Indian defense section is developing light weight aircraft called Light Combat Aircraft (LCA). This aircraft engine's rotating speed lies between 6000rpm and 24000rpm. In aircrafts, 3-5 KVA generator or battery provides power supply to various loads. This aircraft loads require a power supply of 115V to 28 V with a frequency of 100Hz to 400Hz. If this supply system is not working, the backup supply system called Integrated Generator System (IGS) provides power supply to emergency loads present in the aircrafts. The structure of IGS is shown in the figure 1[1-3]. IGS comprises 3 generators, namely PMSG, Inverted Synchronous Generator (ISG) and Synchronous Generator (SG) on a single shaft. The main role of PMSG in this system is to provide excitation to field winding of BG. The main advantages of the permanent magnet machines is the absence of field excitation and field excitation losses, high efficiency, high torque and output power per volume, compactness and better dynamic performance [4]. Due to the introduction of high energy density magnets has allowed the achievement of extremely high flux densities in the PMSG generator; therefore rotor vibration and also reduces the rotation speed of the generator during starting conditions; it cannot be eliminated completely in the PMSG but cogging torque can be minimized in generator [6-7]. There are 5 types of PM machines based on magnet placement in rotor. They are surface winding is not required [5]. PMSG also has some drawbacks like Cogging torque; it is a torque which produces noise mounted magnets, buried magnet (or interior type), rotor with inset surface magnets, V shaped internal magnets and a rotor with radial arrangement internal magnets.

In this, Interior Permanent Magnet Synchronous Machine (IPMSM) has the advantage of high flux concentration & air gap flux density, more sinusoidal current and smooth torque development [8-9]. In buried magnet type motor, the dove tail shaped magnet poles provide better mechanical stability compared

with V shaped magnet poles. Compared with the other types of magnets, rotor buried magnet has less stator filed reaction and slotting effect on magnets. So it has less eddy current losses and high efficiency at high speed of operation. The FEM based buried magnet type PMSG for medium speed application is discussed in [10]. The mechanical stability comparison between surface mounted and buried type PMSG for high speed application is presented in [11] based on FEM analysis. In [12-13], the mathematical modeling of surface mounted and buried type PMSG is given.

None of the works cited in the literature dealt with the coupled electromagnetic field and thermal analysis of spoke type PMSG for high speed application with constrained dimension. This work describes the FEM based performance analysis of the 57 W/19V, 9500 RPM spoke magnet type PMSG for aircraft application with constrained dimension and high speed operation. The second section of this report deals with the modeling of PMSG and the third section presents the simulation analysis. The fourth section concludes the report.

## 2. Mathematical Modeling of S-PMSG

In this section, the analytical modeling of spoke type PMSG is presented. The stator model of the generator is given in [14]. The RMS generated voltage/phase in PMSG is given by

$$E_{ph1} = 4.44 f N_{ph} K_{w1} \Phi_{pm} \quad (1)$$

Where, f is the frequency of the induced voltage in PMSG, in Hz,  $N_{ph}$  is no. of turns in the stator coils per phase,  $K_{w1}$  is fundamental harmonic winding factor,  $\Phi_{pm}$  is flux per pole of the permanent magnet in weber.

Armature MMF is given by

$$\%F = \frac{3 I_{ph} \sin \phi N_{tc} N_{cp}}{2 A P} \quad (2)$$

Where,  $I_{ph}$  is phase current in amps,  $N_{tc}$  and  $N_{cp}$  are number of turns per coil and number of coils per pole respectively,  $\Phi$  is

power factor angle,  $A$  is the number of parallel paths, and  $P$  is the number of rotor poles.

The state vector form of the stator voltages in general can be expressed as in Eq. (3),

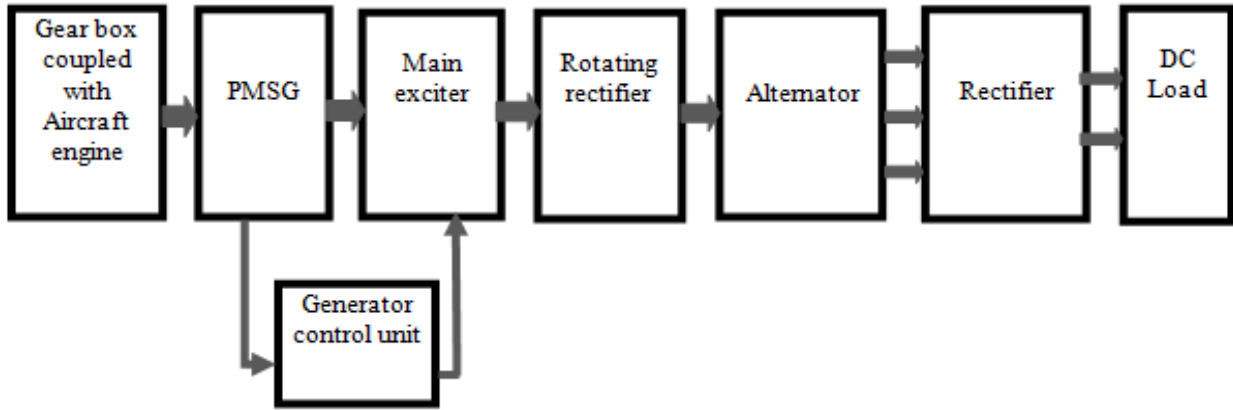


Fig. 1: Structure of IGS

$$V_{abc} = R_s I_{abc}^s + \frac{d\lambda_{abc}^s}{dt} \quad (3)$$

The stator voltage equations in synchronous reference frame are given in Eqns. (4) & (5) respectively for d-axis and q-axis.

$$V_d^s = R_s i_d^s + \frac{d\lambda_d^s}{dt} - \omega_e \lambda_q^s \quad (4)$$

$$V_q^s = R_s i_q^s + \frac{d\lambda_q^s}{dt} - \omega_e \lambda_d^s \quad (5)$$

The expressions for flux linkage are

$$\lambda_d^s = L_d i_d^s + \lambda_m \quad (6)$$

$$\lambda_q^s = L_q i_q^s \quad (7)$$

The spoke magnet rotor modeling is given in [12]. The artificial ring equivalent mass density is

$$P_{sequ} = p_{Fe} \frac{A_m + A_{Fe}}{A_{sequ}} \quad (8)$$

Where  $p_{Fe}$  is mass density of the back iron,  $A_m$  is the area of magnet,  $A_{Fe}$  is the area of the back iron and  $A_{sequ}$  is the area equivalent ring.

The tangential stress of the ring due to rotational speed is

$$\sigma_{t,sequ} = \left( \frac{r_{sequ,r} + r_{sequ,i}}{2} \right)^2 \omega^2 P_{sequ} \quad (9)$$

The analytical design parameters of the stator and the Inset type Permanent Magnet in rotor are calculated based on the standard design equation available in the [15-16]. The design specification for the stator and the rotor are listed in table 1.

Table 1: Stator Parameter Values

Parameter	Value
Stator Outer Diameter, (mm)	108
Stator inner diameter ,(mm)	80
Stator Tooth Width, Wts (mm)	8.6
Air gap length, $L_g$ (mm)	0.6
Number of Slots, S	9
Stator Turns/Phase	126

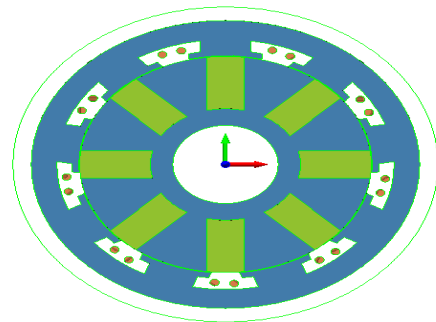
Slot Type	L
Stator copper mass, Kg	0.133
Conductors Used in Stator, (SWG)	21*1
Rotor Outer Diameter, (mm)	78.5
Number of Poles, P	8
Rotor inner diameter , (mm)	74.5
Number of parallel paths	1
Magnet dimension,(mm)	24 x 4

### 3. Simulation Analysis

This section presents the simulation of the analytically designed Inset type Permanent Magnet Synchronous Generator by finite element analysis (FEA). Electromagnetic field analysis is carried out using MagNet software version 7.2. Thermal analysis of S-PMSG is carried out using ThermNet software. This FEA analysis is used to design and simulate complicated structure with non-linear elements.

#### 3.1. Electromagnetic Field Analysis of Spoke Type PMSG

In FEA the entire system is divided into finite elements called meshes with each mesh being solved separately and integrated to the entire machine. The electromagnetic field analysis is carried out using MagNet software. In the preprocessor analytically calculated S-PMSG is designed ; it has 9 stator slots with Cold rolled steel material; the rotor core material carries cold rolled steel material; permanent magnet of samarium cobalt is inset in the core of the rotor. The post processor carries simulation of static, mesh and transient 2d analysis for the time period of ten seconds with time step of one. The solid model and mesh structure of the S-PMSG is shown in figure 2. The PMSG has a mesh size of 2mm.



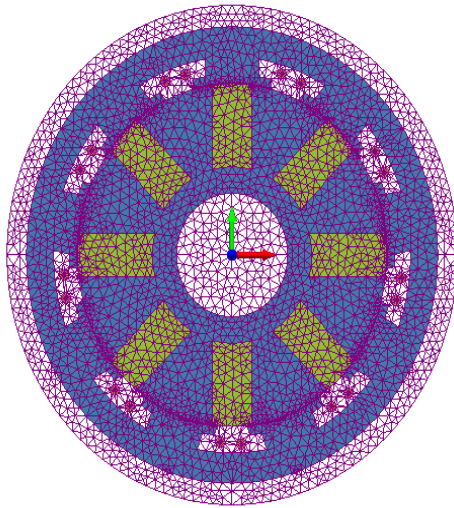


Fig. 2: Solid model and mesh structure of S-PMSG

The developed S-PMSG is to provide output of 57 W/ 19 V at 9500 RPM with single layer distributed type winding. In single layer winding, the concentrated type with 120 degree phase shift has to be wound without any over lapping of winding for all the three phases [R,Y,B]. Calculation for winding is carried out [8] slots per pole ratio ( $9/8=1.2$ ), but in the distributed winding calculation is carried out by using slots per pole ratio. Distributed winding has greater efficiency than the concentrated winding, because it increases the ohmic losses and decreases the eddy current losses at high speed operation. Figure 3 shows three phase winding arrangements. Concentrated winding configuration is shown in table 2.

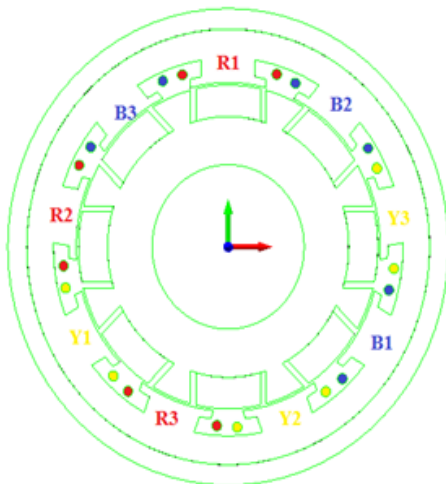


Fig. 3: Stator winding Connection

Table 2: Concentrated Winding Configuration

Phase	Total number of stator slots								
	Slot number								
	1	2	3	4	5	6	7	8	9
R,Y,B	R1	B3	R2	Y1	R3	Y2	B1	Y3	B2

In static analysis, the static flux linkage of the generator is obtained and it is shown in figure 4. The maximum static flux linkage value is  $0.0035\text{Wb/m}^2$ . Cogging torque analysis in FEM analysis is carried out during static analysis of machine. The static torque of machine is obtained by changing rotor position from zero to 360 degree and rotor rotation speed equals zero. Cogging torque of maximum 0.1 Nm occurs in the S- PMSG which is shown in figure 5.

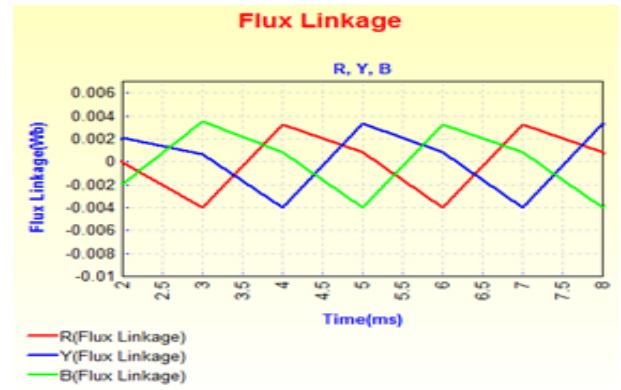


Fig. 4: Flux linkage at static condition



Fig. 5: Cogging Torque

Transient performance of S-PMSG is simulated for a time period of 10 seconds, with time step of 1. Designed S-PMSG rotates at 9500 RPM with distributed winding. The parameters fixed for this electromagnetic field transient analysis are given in table 3.

Table 3: 2D Electromagnetic Field Transient Simulation Parameter

Parameter	Value
Number of steps	10
Iterative Method	Newton Raphson Method
Newton Tolerance	1%
Maximum Newton Iterations	20
Adaption	P - Type
Speed in rpm	9500
Mesh size in mm	2
Solver Type	Transient 2D with motion

From simulation analysis, we find that the generator produces maximum flux linkage of  $2.116\text{Wb/m}^2$ , flux distribution is more uniform, and no leakage flux occurs in the outer periphery which is shown in figure 6. Figure 7 shows the maximum no load voltage of 10 Volts and load current as 6 Amps & the wave form is slightly non sinusoidal because of the presence of cogging torque.

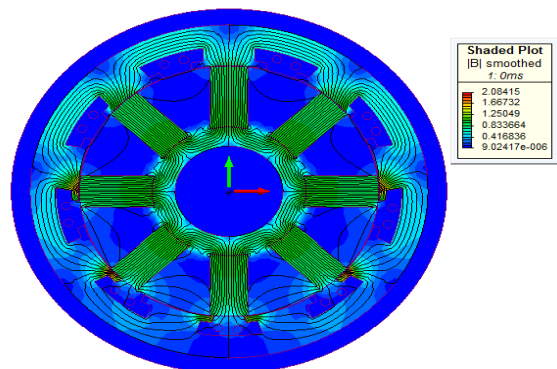


Fig. 6: Flux distribution of S-PMSG at 9500 RPM

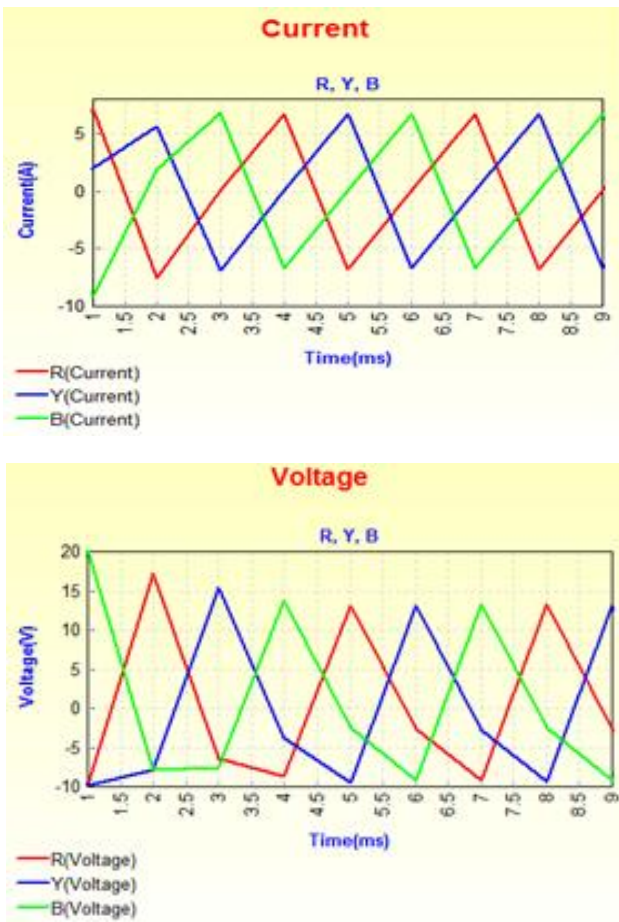


Fig. 7: No load Voltage & Load current of S-PMSG at 9500 RPM

The Generator Control Unit requires DC power, so S-PMSG output is in the form of AC; AC output is converted into DC by connecting diode bridge rectifier in the new circuit window; it is available in the MagNet software itself, armature windings are connected with the diode bridge rectifier along with the resistive load of 3.2 Ohms which is shown in figure 8; it produces DC output voltage and current in the load side. Inset type Permanent Magnet Synchronous Generator running at 9500 RPM produces Maximum DC output voltage of 19 Volts as shown in figure 9 and the DC current of 3 Amps is shown in figure 9. The power it generates in the load is suitable for aircraft to perform at high speed operation.

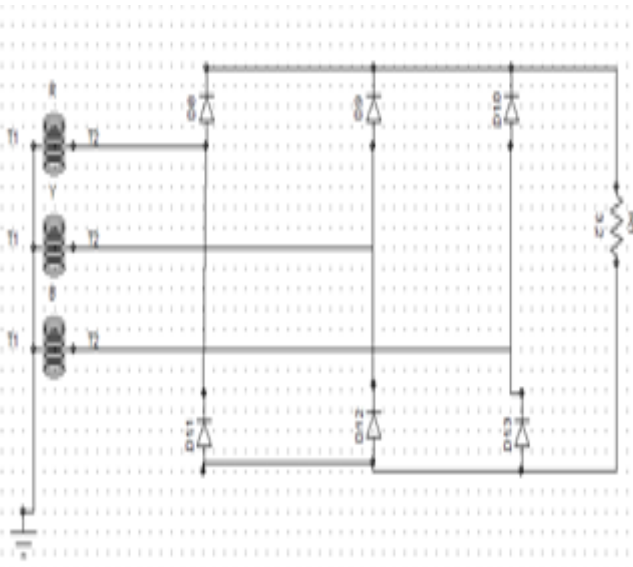


Fig. 8: S-PMSG connected to rectifier through load

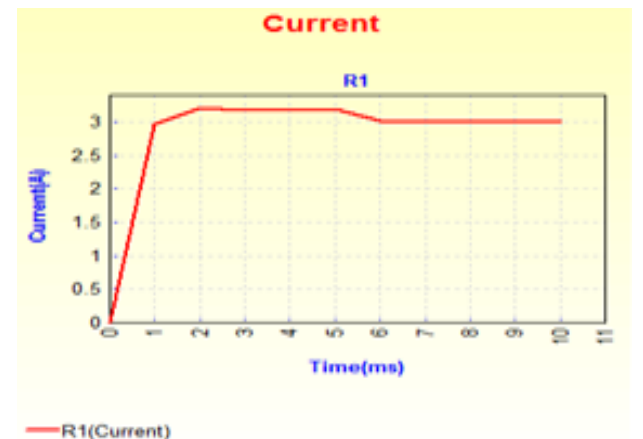
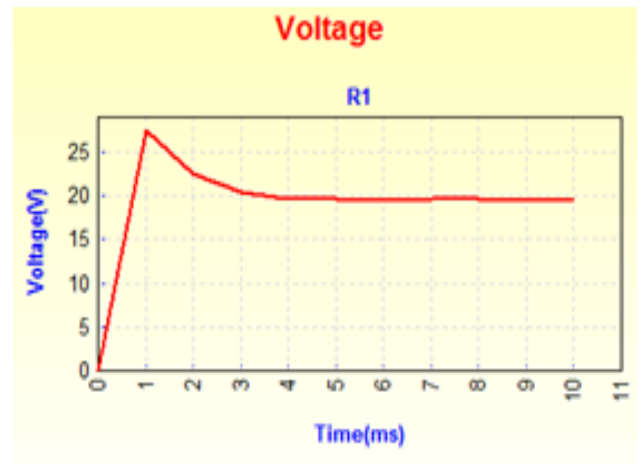


Fig. 9: DC load voltage and load current

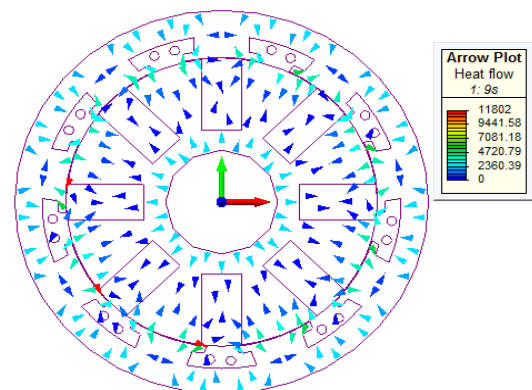
### 3.2. Thermal Analysis of S-PMSG

Thermal analysis of PMSG is simulated using ThermNet software. The parameters fixed for performing thermal transient analysis is given in table 4.

Table 4: 2D Thermal Simulation Parameter

Parameter	Value
Surrounding Temperature	20°C
Thermal heat transfer coefficient	75W/m <sup>2</sup> °C
Emissivity	0.999
No on boundary conditions	3
Solver type	Transient 2D

Temperature of a machine is obtained for a time period of 50ms. From the transient temperature model, the core of the rotor and the edges of the salient stator teeth carry more heat of 32.2°C as shown in figure 10. The heat flow plot is shown in figure 10.



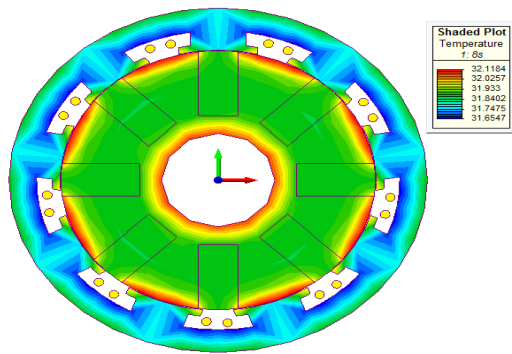


Fig. 10: Temperature Plot of S-PMSG

The results obtained from the simulation analysis are given in table 5. From the static, transient and temperature simulation for the concentrated type Inset type PMSG it produces a maximum of 68 Watts power during 9500 RPM and the cogging torque presence in this Inset type PMSG is 0.1 Nm. Also it affects the output voltage during no load condition. Temperature of this constrained dimension produces 21.26°C during 9500 RPM and it does not cross the 30 degree Celsius limit, so it is safer to operate at high speed and constrained dimension.

Table 5: Simulation Output Performance

Parameter	Unit	Simulation Output
Power	Watts	57
Speed	RPM	9500
DC voltage	Volts	19
DC current	Amps	3
Cogging torque	Nm	0.1
Temperature	°C	32.2
Losses	Watts	25.28
Efficiency	Percentage	82.3

#### 4. Conclusion

This paper has presented Electromagnetic field, thermal and cogging torque analysis for aircraft Integrated Generator System for backup power supply. The electromagnetic field analysis has shown that this Inset type PMSG produces a power of 57 W for Generator control Unit with less temperature rise during high speed operation of 9500 RPM; finally, the cogging torque that occurs in this machine is less and it does not affect the performance of the machine very much, so it can be stated here that the designed Inset type PMSG is suitable for operating at high speed applications with constrained dimension. It can also be used for marine, wind, flywheels etc.

The hardware implementation and cogging torque reduction of the generator will be studied in the future.

#### References

- [1] Deepak Arumugam, Premalatha Logamani and Santha Karuppiah, "Improved Performance of integrated generator system with claw pole alternator for aircraft applications", Elsevier Energy, <http://dx.doi.org/10.1016/j.energy.2017.05.132>, pp-808-821, 2017.
- [2] Deepak Arumugam, Premalatha Logamani and Santha Karuppiah, "Design and implementation of claw pole alternator for aircraft application", Applied Computational Electromagnetic fields Society Journal, Vol. 31, No.5, pp-582-585, 2016.
- [3] Nicolas Patin, Lionel Vido, Eric Monmasson Jean-Paul Louis, Mohamed Gabsi, and Michel Lecrivain, "Control of a hybrid excitation synchronous generator for aircraft applications", IEEE Transactions on Industrial Application, Vol. 55, No. 10, pp-3772-3782, 2008.
- [4] Themistoklis Kefalas, George Kalokiris, Antonios Kladas and John Tegopoulos, "Design of skewed mounted permanent magnet synchronous generators based on 2D and 3D finite element techniques", Journal of Materials Processing Technology, pp-288-293, 2005.

- [5] Michael W. Degner, Richard Van Maaren, Azza Fahim, Donald W. Novotny, Robert D. Lorenz and Charles D. Syverson, "A Rotor Lamination Design for Surface Permanent Magnet Retention at High Speeds" IEEE Transactions On Industry Applications, Vol. 32, No. 2, pp.380-385, 1996.
- [6] Levin N, Orloval S, Pugachov V, Ose Zala B and Jakobsons E, "Methods to reduce the cogging torque in Permanent Magnet Synchronous Machines", Elektronikairelektro tehnika, Vol. 19, No. 1, pp.1-9, 2013.
- [7] Brahim L. Chikouche, Kamel Boughrara and Rachid Ibtouen, "Cogging torque minimization of surface mounted Permanent Magnet Synchronous Machines using hybrid magnet shapes", Progress in electromagnetic fields research, Vol. 62, pp.49-61, 2015.
- [8] Lijunzhou, Yongwei Geng and Zhuoran Zhang, "Comparative study on concentrated winding on permanent magnet synchronous machines with different rotor structures for aircraft generator application", ICEMS, pp-1246-1250, 2015.
- [9] T. F. Chan, L. L. Lai and L. T. Yan, "Performance of a three-phase AC generator with inset NdFeB permanent-magnet rotor", IEEE Transaction on Energy Conversion, Vol. 19, No. 1, pp. 88-94, 2004.
- [10] Jere Kolehmainen and JouniKaheimo, "Motors with Buried Magnets for Medium-Speed Applications", IEEE Transactions on Energy Conversion, Vol. 23, No. 1, pp.86-91, 2008
- [11] Zhang Tao, Ye Xiaoting, Zhang Huiping and Jia Hongyun, "Strength Design on Permanent Magnet Rotor in High Speed Motor Using Finite Element Method", Indonesian Journal of Electrical Engineering, Vol.12, No.3, pp. 1758-1763, 2014.
- [12] Tayfun Gundogdu and Guven Komurgoz, "Design of Permanent Magnet Machines with Different Rotor Type", International Journal of Electrical and Computer Engineering Vol.4, No.10, pp.1510-1515, 2010.
- [13] Bogdan Dumitru Varaticeanu, Paul Minciunescu and Daniel Fodorean, "Mechanical Design and Analysis of a Permanent Magnet Rotors used in High-Speed Synchronous Motor", Electrotehnica Electronica Automatica, Vol. 62, pp.10-17, 2014.
- [14] Paul.C.Krause, Analysis of Electrical Machinery and drive systems, Wiley Publications, 2nd edition, 2000.
- [15] A.K.Sawhney, Course in Electrical Machine design, Dhanpat Rai & Sons publications, 6th edition, 2006.
- [16] J.R.Hendershot and T.J.E.Miller, Design of brushless Permanent Magnet Machines, Oxford Publication, 1st edition, 1995.